Journal of Alloys and Compounds, 186 (1992) 53–64
JALCOM 251

^{47}Ti and ^{49}Ti nuclear magnetic resonance in TiH_2

B. Nowak, O. J. Żogał and K. Niedźwiedź
Institute for Low Temperature and Structure Research, Polish Academy of Sciences, P.O. Box 937, 50-590 Wrocław (Poland)

(Received October 2, 1991; in final form December 20, 1991)

Abstract

The NMR of ^{47}Ti and ^{49}Ti has been observed in TiH_2 in the temperature range 155–310 K. The Knight shift and spin–lattice relaxation rate $(T_1T)^{-1}$ were found to be temperature dependent. The shift varied from $0.245 \pm 0.002\%$ at 310 K to $0.319 \pm 0.002\%$ at 155 K, whereas T_1T varied from 22 ± 1 s K at 310 K to 48.8 ± 3 s K at 155 K. From the temperature dependences of Knight shift and magnetic susceptibility a core polarization hyperfine field of $-(126 \pm 8)$ kOe was deduced. Applying the tight binding approximation the data for the cubic phase (310 K) have been partitioned into spin (s,p,d) and orbital (p,d) contributions.

In the tetragonal phase (below 310 K) a temperature dependence of the d band density of states at the Fermi level was deduced. An influence of the lower symmetry on the spin–lattice relaxation behaviour is discussed.

1. Introduction

As a part of our continuous investigation of NMR in the dihydride phases of transition metals and their alloys [1–7], we have studied the ^{47}Ti and ^{49}Ti NMR in TiH_2. The measurements of the Knight shift K and nuclear spin–lattice relaxation rate $(T_1T)^{-1}$ of transition metal hydrides can give information about their electronic structure at the Fermi level which is difficult to obtain by other experimental methods. To date, however, most experimental efforts for TiH_x hydride phase have been concerned with ^{1}H NMR [8–11].

Most valuable information on electronic structure can be obtained when both components of a binary hydride are accessible to the NMR technique. Such an opportunity appears in the cases of YH_2 [12, 13], ScH_2 [2], VH_2 [3, 4] and NbH_2 [5], where NMR experiments for ^{1}H as well as for the ^{89}Y, ^{45}Sc, ^{51}V and ^{93}Nb have been performed. All these nuclei are about 100% abundant and, although ^{45}Sc, ^{51}V and ^{93}Nb nuclei possess quadrupolar moment, their resonances could be relatively easily observed because of the cubic structure of their dihydrides.

The important contributions to the observed relaxation rates and Knight shifts of metal nuclei in these dihydrides have been shown to arise mainly from orbital and core-polarization hyperfine interactions with the d component of the conduction electron wave functions at the Fermi level.

The NMR active isotopes of titanium, zirconium and hafnium all possess low natural abundance, relatively small gyromagnetic ratio and simultaneously

0925-8388/92/$5.00 © 1992 – Elsevier Sequoia. All rights reserved

a rather large quadrupolar moment. For this reason, it has not yet been possible to observe ^{177}Hf resonance in HfH_2, and that of ^{91}Zr in tetragonal ZrH_2 was detected only fairly recently (by Żogał *et al.* [14]). To our knowledge, there have been only two experiments referring to the ^{47}Ti and ^{49}Ti resonance in TiH_2 [15, 16]. Because of the poor experimental resolution achieved by Frisch and Forman [15], they could not resolve the separate ^{47}Ti and ^{49}Ti lines and therefore could only give a crude estimation of titanium Knight shift. Goren *et al.* [16] observed close-lying ^{47}Ti and ^{49}Ti resonances in TiH_2 in both cubic and tetragonal phases. The Knight shift was measured as a function of temperature for TiH_2 and as a function of hydrogen concentration in TiH_x.

In the present study the temperature dependences of the ^{49}Ti Knight shift and spin–lattice relaxation rates have been measured in TiH_2. The aim of this work is to provide some comprehensive conclusions on the electronic structure and the nature of hyperfine interactions in both the cubic and tetragonal phases of TiH_2. The results are compared with those obtained from specific heat [17, 18], magnetic susceptibility [19] and recent theoretical predictions [20–25]. Of particular interest are questions related to interference effects in the relaxation rate due to possible s–d mixing. They can arise because of the lower-than-cubic symmetry of the tetragonal phase. The contribution of the p symmetry electronic states to the relaxation rate is taken into account; a term which has not been considered previously in the analysis of the spin–lattice relaxation times for the hydrides is also discussed.

2. Experimental procedure

The TiH_2 sample, which was fine powder, was obtained from the Fluke AG, Buchs SG (Switzerland). According to the supplier, the major impurities are: nitrogen, 0.1% or less; chlorine, 0.08% or less; carbon, 0.03% or less; silicon, 0.05% or less; iron, 0.09% or less; nickel, 0.05% or less; and magnesium, 0.04% or less. The sample was checked by X-ray diffraction (at room temperature) to be single phase and the f.c.c. structure was identified with the lattice parameter $a = 4.452 \pm 0.004$ Å. The observed breadths of the X-ray diffraction peaks, however, do not exclude possible small tetragonal deformations at this temperature.

The ^{47}Ti and ^{49}Ti resonances were observed at a resonance frequency of 16.924 MHz on a Bruker MSL 300S spectrometer equipped with a B-VT 1000 E temperature controller. The temperature was varied from 155 to 310 K. The lower value was limited by our present instrumentation and the higher value corresponds to the temperature region where a diffusional contribution to the relaxation is still inefficient.

The spectra obtained are Fourier transforms of typically 2000 signals of free induction decays after a single pulse (5.25 μs). The 90° pulse was adjusted using a $TiCl_4$ reference sample. The dead time of the receiver was about 200 μs for 2000 scans. The spin–lattice relaxation times T_1 were

measured using a 180°–90° pulse sequence. The Knight shifts were measured relative to $TiCl_4$.

3. Experimental results

Figure 1 shows the ^{47}Ti and ^{49}Ti absorption lines recorded at 294 and 155 K. The two peaks are attributed to the two isotopes, the ^{49}Ti (on the left) having spin $I=7/2$ and ^{47}Ti with $I=5/2$. At 310 K TiH_2 exists as a cubic phase and should not show quadrupolar interaction. It is known that below this temperature the transition to tetragonal phase is observed and the axial ratio c/a decreases with decreasing temperature. Increasing tetragonality induces the stronger quadrupolar interaction and the signal-to-noise ratio decreases at lower temperatures. However, the ^{47}Ti and ^{49}Ti lines are still well resolved at 155 K. The ^{49}Ti resonance was chosen for further analysis of the temperature dependences of both Knight shifts and spin–lattice relaxation times since this resonance is more prominent than that of ^{47}Ti, thus offering a better signal-to-noise ratio.

Figure 2 shows the temperature dependence of the ^{49}Ti Knight shift. The observed lineshapes and temperature dependence of the Knight shift are in full agreement with the data of Goren *et al.* [16]. The presently reported value of $K=0.245\pm0.002\%$ for the Knight shift of the cubic phase (at 310 K) is only slightly lower than the $0.252\pm0.001\%$ obtained by Goren *et al.* [16] for temperatures above 300 K.

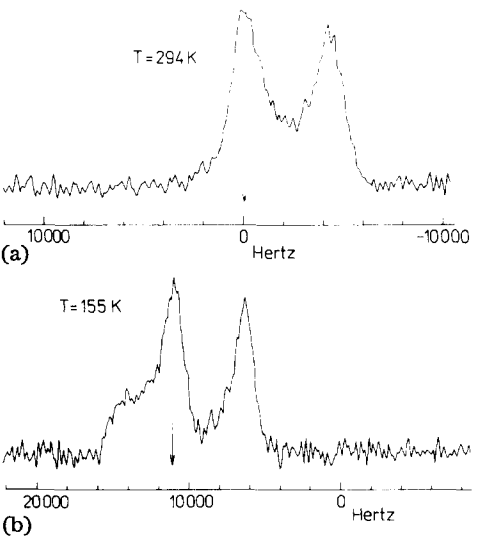

Fig. 1. The absorption spectra of the ^{47}Ti and ^{49}Ti resonances in TiH_2 at (a) 294 K and (b) 155 K. Note that the horizontal scale slightly differs in the two cases. Zeroes on the frequency scale correspond to the ^{49}Ti Knight shift value of 0.254%, measured with respect to the ^{49}Ti signal in $TiCl_4$ at 294 K. The arrows indicate the posiiton of the ^{49}Ti peak used for Knight shift determination.

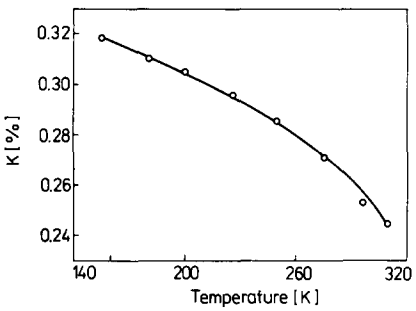

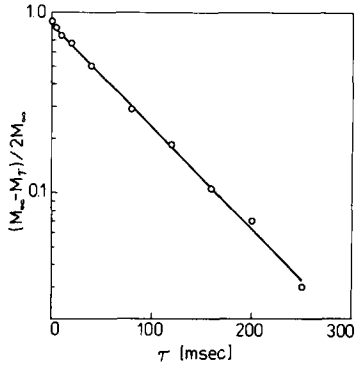

Fig. 2. Temperature dependence of the ^{49}Ti Knight shift in TiH_2.

Fig. 3. Recovery of the ^{49}Ti nuclear magnetization as a function of pulse spacing τ at $T=294$ K.

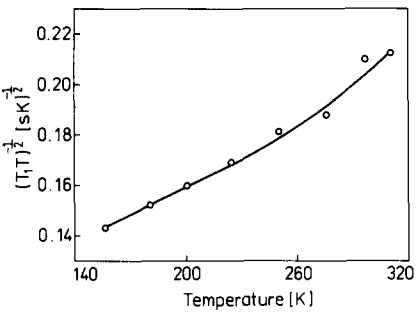

Fig. 4. The $(T_1T)^{-1/2}$ values of ^{49}Ti resonance for temperatures T from 155 to 310 K.

Figure 3 shows an example of the recovery curve of the nuclear magnetization obtained at $T=294$ K. The experimental points are fitted to a straight line. It intercepts the ordinate axis at $[M_\infty - M(\tau)]/2M_\infty < 1$ which indicates the partial saturation of the nuclear spin system. Despite this, the spin–lattice relaxation time was derived from the slope which is consistent with the conclusions of Simmons *et al.* [26].

Figure 4 shows the results of the T_1 measurements on ^{49}Ti. We have plotted $(T_1T)^{-1/2}$ for ^{49}Ti *vs.* temperature to show that its temperature dependence corresponds qualitatively to that of $(T_1T)^{-1/2}$ for ^{1}H reported in refs. 8, 10 and 11.

4. Discussion

4.1. Cubic phase

In the cubic phase, since s, p and d functions belong to different irreducible representations of the cubic group, the relaxation rate is given by a sum of the individual hyperfine contributions [27]:

$$(T_1T)^{-1} = 4\pi\hbar\gamma^2 k_B\{[N_s(0)H_s^F]^2 + [N_p(0)H_p^{orb}]^2 F_p^{orb} + [N_p(0)H_p^{orb}]^2 F_p^{dip} + [N_d(0)H_d^{orb}]^2 F_d^{orb} + [N_d(0)H_d^{orb}]^2 F_d^{dip} + [N_d(0)H_d^{cp}]^2 F_d^{cp}\} \quad (1)$$

where $\hbar = h/2\pi$ is Planck's constant; γ is the nuclear gyromagnetic ratio; k_B is Boltzmann's constant; $N_s(0)$, $N_p(0)$ and $N_d(0)$ are the densities of states at the Fermi energy from the s, p and d bands respectively for one direction of the spin. H_s^F, H_p^{orb}, H_d^{orb} and H_d^{cp} are the s–Fermi contact, p orbital, d orbital and d core polarization hyperfine fields respectively. Finally, F_p^{orb}, F_p^{dip}, F_d^{orb}, F_d^{dip} and F_d^{cp} are the reduction factors, which arise from the orbital degeneracy of the p and d bands. In the case of cubic transition metals $F_p^{orb} = 2/9$, $F_p^{dip} = 1/15$ and F_d^{orb}, F_d^{dip} and F_d^{cp} are functions of a single parameter $f(t_{2g})$ indicating the degree of admixture of t_{2g} and e_g character of the d functions at the Fermi level:

$$F_d^{orb} = \frac{2}{3} f(t_{2g}) \left[2 - \frac{5}{3} f(t_{2g}) \right] \quad (2)$$

$$F_d^{dip} = \frac{1}{147} \{5[f(t_{2g})]^2 - 6f(t_{2g}) + 6\} \quad (3)$$

$$F_d^{cp} = \frac{1}{3} [f(t_{2g})]^2 + \frac{1}{2} [1 - f(t_{2g})]^2 \quad (4)$$

In analysing the Knight shift K and the molar magnetic susceptibility χ in the 3d transition metals several contributions must be considered in addition to the diamagnetic terms: that of the usual s conduction electron susceptibility χ_s and the resulting Fermi contact hyperfine shift K_s^F, as well as two contributions arising from the presence of d electrons, the spin paramagnetic susceptibility of the unfilled 3d conduction band χ_d and the resulting induced polarization of the core electrons, with the associated shift K_d^{cp}, and lastly the Van Vleck orbital susceptibility of the partially filled 3d band χ_d^{VV}, and the resulting shift K_d^{VV}. A negligibly small core polarization comes from the s and p conduction bands and they will be omitted in following expression for the observed Knight shift:

$$K_{obs} = K_{dia} + K_s^F + K_d^{cp} + K_d^{VV} = \frac{2}{N} \frac{\langle r^{-1} \rangle}{\langle r^2 \rangle} \chi_{dia} + (\mu_B N)^{-1} [H_s^F \chi_s + H_d^{cp} \chi_d + H_d^{VV} \chi_d^{VV}] \quad (5)$$

and

$$\chi_{obs} = \chi_{dia} + \chi_s + \chi_p + \chi_d + \chi_d^{VV} \quad (6)$$

$$\chi_s = 2\mu_B^2 N_s(0) \quad (7)$$

$$\chi_p = 2\mu_B^2 N_p(0) \quad (8)$$

$$\chi_d = 2\mu_B^2 N_d(0)[1 - V_C N_d(0)]^{-1} \quad (9)$$

In these equations N is Avogadro's number, μ_B is the Bohr magneton, V_C is the effective Coulomb potential which enhances the d band spin susceptibility over the value given by the free electron approximation, H_d^{VV} is the d orbital hyperfine field. It should be pointed out that H_d^{orb} in eqn. (1) represents an average over the Fermi surface, while the H_d^{VV} in eqn. (5) is weighted over all states which contribute to χ_d^{VV}. Finally, $\langle r^2 \rangle$ and $\langle r^{-1} \rangle$ are the average nth power of the electron orbital radius.

The diamagnetic contribution to the titanium Knight shift can be estimated from the approximate expression [28]

$$K_{dia}(\%) = -100\Delta n r_0/a_0 \tag{10}$$

where Δn represents the difference in 3d electron occupancy between the shift reference and the hydride, and r_0 and a_0 are the classical electron radius and the first Bohr radius respectively. In the case of TiH_2 the shift is measured with respect to $TiCl_4$, and Δn is about 2, thus giving $K_{dia} \approx -0.01\%$. The diamagnetic contribution to the observed molar susceptibility χ_{dia} was then evaluated using $\langle r^{-1} \rangle$ and $\langle r^2 \rangle$ values given for Ti^{2+} ($3d^2$) by Freeman and Watson [29] and we have obtained $\chi_{dia} \approx -10 \times 10^{-6}$ e.m.u. mol^{-1}.

Before the above equations can be used for further analysis, the values of the appropriate hyperfine fields have to be known. H_d^{cp} can usually be estimated from the plot of Knight shift K *vs.* χ if they both show temperature dependence and if it can be assumed that both temperature dependences are only caused by the d spin contributions. Such an opportunity appears in TiH_2 where, using the present Knight shift data and magnetic susceptibility data of Trzebiatowski and Staliński [19], we have obtained $H_d^{cp} = -(0.126 \pm 0.008) \times 10^6$ Oe (Fig. 5). This value is very close to $H_d^{cp} = -0.118 \times 10^6$ Oe calculated for h.c.p. titanium metal by Asada and Terakura [30]. We note at this point that Goren *et al.* [16], combining their titanium Knight shift data and proton spin–lattice relaxation rate data with the theoretical data on $N(0)$ reported by different authors, have estimated H_d^{cp} to be 0.154×10^6 Oe $< |H_d^{cp}| < 0.313 \times 10^6$ Oe.

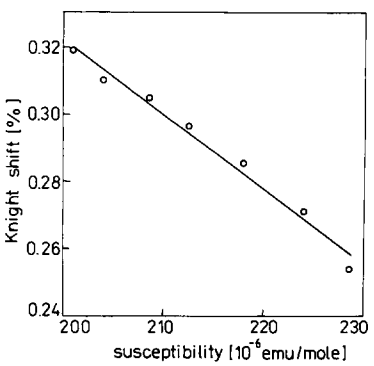

Fig. 5. The ^{49}Ti Knight shift K *vs.* magnetic susceptibility χ, with temperature as the implicit parameter. $\chi(T)$ was taken from the work of Trzebiatowski and Staliński [19].

The values of hyperfine fields we have used in the present analysis are given in Table 1. H_s^F, H_p^{orb} and H_d^{orb} are taken to be the same as those calculated for h.c.p. titanium metal by Asada and Terakura [30]. Ebert *et al.* [31] have approximated H_d^{VV} by $0.85H_d^{orb}$ in their analysis of titanium Knight shift in h.c.p. titanium and we adapted this approximation in K for our case of TiH_2.

The band structure calculations for cubic titanium-rich $Ti_{1-x}Nb_x$ [25] dihydrides showed that the partial wave components of the electron densities of states are $N_s(0):N_p(0):N_d(0) \approx 1:8:91$. These ratios are nearly independent of x (see, for example, ref. 25, Table 2). We have used them in our partitioning procedure for the cubic TiH_2. The t_{2g} character of the titanium d electron functions at the Fermi energy increases with decreasing concentration of niobium [25]. When $x \to 0$ we obtain $f(t_{2g}) \approx 0.56$. The remaining parameter is $N(0)$ which we have adjusted to give an agreement between the calculated and observed relaxation rates. Our evaluation of $N(0) = 1.121$ states $(eV)^{-1}$ compares favourably with that derived from the ^{93}Nb Knight shift and relaxation rate analysis in $Ti_{0.95}Nb_{0.05}H_{1.94}$ [1] and falls in between the theoretically calculated $N(0) = 0.85$ states $(eV)^{-1}$ [23], 0.95 states $(eV)^{-1}$ [21], 1.03 states $(eV)^{-1}$ [24], 1.33 states $(eV)^{-1}$ [22] and 1.73 states $(eV)^{-1}$ [20] for TiH_2.

The estimated contributions of s, p and d bands to $N(0)$ and $(T_1T)^{-1}$ are given in Table 1. It is apparent that the dominant relaxation process arises from the d orbital contribution. This conclusion is insensitive to possible errors in assumed values of the hyperfine fields. Subtracting the diamagnetic

TABLE 1

^{49}Ti magnetic hyperfine fields and conduction electron contributions to the total density of states, and spin–lattice relaxation rate, in the cubic phase of TiH_2[a]

Parameter	Source	Value
H_s^F		4.993×10^6 Oe
H_p^{orb}		0.916×10^6 Oe
H_d^{orb}		0.21×10^6 Oe
H_d^{VV}		0.179×10^6 Oe
H_d^{cp}		-0.126×10^6 Oe
$N_s(0)$		0.011 states $(eV)^{-1}$ $(spin)^{-1}$
$N_p(0)$		0.09 states $(eV)^{-1}$ $(spin)^{-1}$
$N_d(0)$		1.02 states $(eV)^{-1}$ $(spin)^{-1}$
$f(t_{2g})$		0.56
V_C		0.34 eV
$(T_1T)^{-1}$	s	0.0051 s^{-1} K^{-1}
	p_{orb}	0.0024 s^{-1} K^{-1}
	p_{dip}	0.0007 s^{-1} K^{-1}
	d_{orb}	0.0296 s^{-1} K^{-1}
	d_{dip}	0.0022 s^{-1} K^{-1}
	d_{cp}	0.0054 s^{-1} K^{-1}

[a]Based on the procedure described in the text.

TABLE 2

The Knight shifts and magnetic susceptibility partitioned into their different terms[a]

Parameter	Source	Value
K (%)	s	0.064
	d (Van Vleck)	0.419
	d_{cp}	−0.228
	Diamagnetism	−0.01
χ ($\times 10^{-6}$ e.m.u. mol^{-1})	s spin	0.7
	p spin	5.8
	d spin	100.9
	d orbital	130.6
	Diamagnetism	−10.0

[a]Obtained as described in the text.

and s and p contributions to the magnetic susceptibility and Knight shift from the measured values and combining eqns. (5), (6) and (9), we have found the d spin and d orbital contributions as well as the magnitude of V_C. Numerical data are presented in Tables 1 and 2. Again, the orbital contributions dominate in both the Knight shift and the susceptibility.

Additional verification of our estimate of the temperature-independent magnetic susceptibility contributions χ_s, χ_p and χ_{VV} can be made by comparison of the experimental susceptibility at about 0 K with the calculated value. Subtracting $N_s(0)+N_p(0)=0.101$ states (eV)$^{-1}$ from $N(0)=0.71$ states (eV)$^{-1}$ evaluated by Bohmhammel *et al.* [18] from the low temperature specific heat measurements for $TiH_{1.99}$ we obtain $N_d(0)=0.609$ states (eV)$^{-1}$ and from eqn. (9) $\chi_d(0\ K)=49.7\times10^{-6}$ e.m.u. mol^{-1}. Hence $\chi_{calc}(0\ K)=\chi_{dia}+\chi_s+\chi_p+\chi_d+\chi_{VV}=(-10+0.7+5.8+49.7+130.6)\times10^{-6}=176.8\times10^{-6}$ e.m.u. mol^{-1}. The magnetic susceptibility data of Trzebiatowski and Staliński for $TiH_{1.98}$ [19] extrapolated to 0 K give $\chi_{obs}\approx190\times10^{-6}$ e.m.u. mol^{-1}, which compares favourably with that calculated above.

4.2. Tetragonal phase

For the tetragonally deformed CaF_2-type structure of TiH_2, the appropriate point group is D_{4h} (4/*mmm*) on the titanium sites. For the D_{4h} local symmetry the s-like ($l=0$) atomic function transforms as the A_{1g} representation; the three p-like ($l=1$) and five d-like ($l=2$) functions from bases for irreducible representations A_{2u}, E_u, A_{1g}, B_{1g}, B_{2g} and E_g respectively. Since both $s(Y_0^0)$ and $s(Y_2^0)$ functions belong to the A_{1g} representation, the resulting (negative) interference term between Fermi contact and core polarization interactions must be added to eqn. (1). The p and d dipolar contributions to the relaxation rate are small, as in the case of cubic phase, and therefore will be ignored in the following. Using the calculation procedure described by Narath [32] and Asada and Terakura [30], we obtain a $(T_1T)^{-1}$ formula appropriate for the tetragonal phase and powder sample:

$$(T_1T)^{-1} = 4\pi\hbar\gamma^2 k_B\{[N_s(0)H_s^F]^2 + [N_p(0)H_p^{orb}]^2 F_p'^{orb} + [N_d(0)H_d^{orb}]^2 F_d'^{orb} + [N_d(0)H_d^{cp}]^2 F_d'^{cp} + 2H_s^F H_d^{cp}|\Omega_{sd}^{A_{1g}}(0)|^2\} \quad (11)$$

with

$$F_p'^{orb} = \frac{4}{3}f(A_{2u})f(E_u) + \frac{2}{3}f^2(E_u) \quad (12)$$

where

$$2f(E_u) + f(A_{2u}) = 1 \quad (13)$$

and

$$F_d'^{orb} = \frac{4}{3}f(E_g)[6f(A_{1g}) + f(B_{1g}) + f(B_{2g}) + \frac{1}{8}f(E_g)] \quad (14)$$

$$F_d'^{cp} = f^2(A_{1g}) + f^2(B_{1g}) + f^2(B_{2g}) + \frac{1}{2}f^2(E_g) \quad (15)$$

where

$$f(A_{1g}) + f(B_{1g}) + f(B_{2g}) + 2f(E_g) = 1 \quad (16)$$

It is evident from the above equation that the correction factor $F_p'^{orb}$ is a function of a single parameter whereas $F_d'^{orb}$ and $F_d'^{cp}$ become functions of three independent parameters expressing the relative weights of admixture among A_{1g}, B_{1g}, B_{2g} and E_g symmetry types of d functions at the Fermi level. The quantity $\Omega_{sd}^{A_{1g}}(0)$ in eqn. (11) is the so-called off-diagonal density of states at the Fermi energy, discussed for the first time by Asada and Terakura [30] in the case of relaxation rates in h.c.p. transition metals.

Since $|\Omega_{sd}^{A_{1g}}(0)|^2$ does not mean a product $N_s^{A_{1g}}(0)N_d^{A_{1g}}(0)$, it is difficult to predict the behaviour of the off-diagonal density of states from that of the partial density of states.

A slightly different expression for the Fermi contact–core polarization interference term was given by Narath [32] for the case of h.c.p. titanium but we omit the details because of the other complications mentioned above.

Having gained some faith in the spin–lattice relaxation, Knight shift and magnetic susceptibility partitioning for the cubic phase, we now examine the predictions for the tetragonal phase.

Subtracting K_s^F, K_d^{VV} and K_{dia} from the measured shifts we have obtained the core-polarization contribution K_d^{cp} and from eqns. (5) and (9) we have evaluated the densities of states $N_d(0)$ for each measured temperature. Subsequently, we have plotted the experimental values of $(T_1T)^{-1}$ against $N_d^2(0)$ (Fig. 6).

Figure 6 reveals two striking features. In the first place, the experimental rates are seen to be a linear function of $N_d^2(0)$, thus indicating that the magnitude of $4\pi\hbar\gamma^2 k_B[(H_d^{orb})^2 F_d'^{orb} + (H_d^{cp})^2 F_d'^{cp}]$ is temperature independent. Secondly, the point of intersection of that line at $N_d^2(0)$ yields a negative

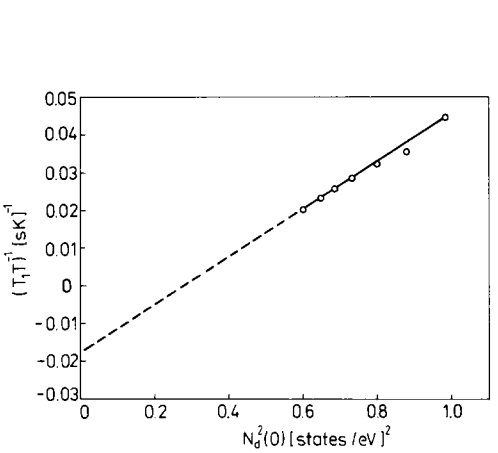

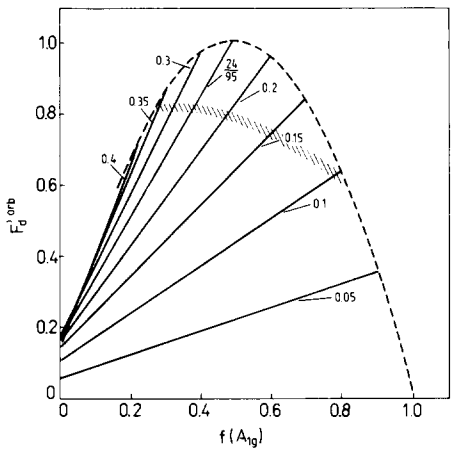

Fig. 6. Plot of $(T_1T)^{-1}$ *vs.* the square of the d band density of states $N_d^2(0)$ for the tetragonal phase of TiH_2.

Fig. 7. Plot of the d orbital reduction factor $F_d^{\prime orb}$ for tetragonal symmetry as a function of the orbital admixture coefficients $f(A_{1g})$ and $f(E_g)$: ——, solutions for given values of $f(E_g)$; – – –, the area of allowed solutions.

value and this shows that the Fermi contact–core polarization interaction coming from an s–d admixture in the A_{1g} representation is an important contribution to the total relaxation rate. Taking eqn. (16) into account the expression for $F_d^{\prime orb}$ can be rewritten in the form

$$F_d^{\prime orb} = \frac{20}{3} f(E_g)\left[\frac{1}{5} + f(A_{1g}) - \frac{3}{8} f(E_g)\right] \tag{17}$$

which clearly shows that $F_d^{\prime orb}$ is independent of the ratio $f(B_{1g})/f(B_{2g})$. Dependence of the $F_d^{\prime orb}$ factor on the orbital admixture coefficients $f(A_{1g})$ and $f(E_g)$ is illustrated in Fig. 7. The shaded area represents a set of solutions for $f(A_{1g})$, $f(E_g)$, $f(B_{1g})$ and $f(B_{2g})$, which reproduce the straight line in Fig. 6. Again, the results suggest a considerable s–d admixture in the A_{1g} representation.

5. Conclusions

For the cubic γ phase of TiH_2 we have partitioned the ^{49}Ti relaxation rate, Knight shift and magnetic susceptibility into s, p and d band contributions. The interactions we investigated include direct Fermi contact, orbital, dipole and core-polarization interactions. We have found that the dominant contributions arise from the d orbital terms. The core-polarization interaction which is responsible for the temperature dependence of the measured Knight shift provides, however, a minor contribution to the relaxation rate. We have shown that the p component, which has so far not been considered in

analysing experiments on the relaxation rates of transition metal hydrides, amounts to about 7% of the total relaxation rate.

The temperature dependences of the ^{49}Ti Knight shift and spin–lattice relaxation (this work) as well as the previously reported data on ^{1}H NMR and magnetic susceptibility [10, 11, 17, 19] provide evidence that the total density of states at the Fermi level in the tetragonal δ phase of TiH_2 is continuously reduced with decreasing temperature. There exists a strong correlation between the splitting of the cubic into tetragonal lattice constants with decreasing temperature and the corresponding changes in the magnetic susceptibility, Knight shifts and spin–lattice relaxation rates. However, at the present stage, it is difficult to draw quantitative conclusions about the experimental dependences because the c/a ratio is temperature dependent, and the bands at the Fermi level are continuously modified by the change in temperature. A detailed assessment must await future calculations that can better describe changes in the band structure with varying lattice constant.

Note added in proof

Very soon after this paper had been accepted, the authors realized that eqns. 14, 15 and 17 were incorrect. Thus, Fig. 7 and the consequences resulting from it are invalid. We hope to present the correct equations for $F_d'^{orb}$ and $F_d'^{cp}$ shortly in this journal.

We are sorry for any inconvenience caused by our delay.

References

1 B. Nowak, O. J. Żogał and M. Minier, *J. Phys. C, 12* (1979) 4591.
2 O. J. Żogał and S. Idziak, *Physica B, 104* (1981) 365.
3 B. Nowak and M. Minier, *J. Phys. C, 15* (1982) 4385.
4 B. Nowak, O. J. Żogał and H. Drulis, *J. Phys. C, 15* (1982) 5829.
5 B. Nowak and M. Minier, *J. Phys. F, 14* (1984) 1291.
6 B. Nowak and M. Minier, *J. Less-Common Met., 101* (1984) 245.
7 B. Nowak, Y. Chabre and R. Andreani, *J. Less-Common Met., 130* (1987) 193.
8 C. Korn, *Phys. Rev. B, 17* (1978) 1707.
9 C. Korn, *Phys. Rev. B, 28* (1983) 95.
10 R. Göring, R. Lukas and K. Bohmhammel, *J. Phys. C, 14* (1981) 5676.
11 R. C. Bowman, Jr., and W. K. Rhim, *Phys. Rev. B, 24* (1981) 2232.
12 D. S. Schreiber, *Phys. Rev., 137* (1965) A860.
13 A. Narath and T. Fromhold, Jr., *Phys. Lett. A, 25* (1967) 49.
14 O. J. Żogał, B. Nowak and K. Niedźwiedź, *Solid State Commun., 80* (1991) 601.
15 R. G. Frisch and R. A. Forman, *J. Chem. Phys., 48* (1968) 5187.
16 S. D. Goren, C. Korn, H. Riesemeier, E. Rössler and K. Lüders, *Phys. Rev. B, 34* (1986) 6917.
17 F. Ducastelle, R. Caudron and P. Costa, *J. Phys. (Paris), 31* (1970) 57.
18 K. Bohmhammel, G. Wolf, G. Gross and H. Mädge, *J. Low Temp. Phys., 43* (1981) 521.
19 W. Trzebiatowski and B. Staliński, *Bull. Acad. Pol. Sci., 1* (1953) 131.
20 M. Gupta, *Solid State Commun., 29* (1979) 47.
21 N. I. Kulikov, *Phys. Status Solidi B, 91* (1979) 753.
22 A. Fujimori and N. Tsuda, *Solid State Commun., 41* (1982) 491.
23 A. C. Switendick, *J. Less-Common. Met., 101* (1984) 191.

24 D. A. Papaconstantopoulos, P. M. Laufer and A. C. Switendick, in G. Bambakidis and R. C. Bowman, Jr., (eds.), *Hydrogen in Disordered and Amorphous Solids*, Vol. 136, Plenum, New York, NY, 1986.
25 D. A. Papaconstantopoulos and P. M. Laufer, *J. Less-Common Met.*, *130* (1987) 229.
26 W. W. Simmons, W. J. O'Sullivan and W. A. Robinson, *Phys. Rev.*, *127* (1962) 1168.
27 A. Narath, in A. J. Freeman and R. B. Frankel (eds.), *Hyperfine Interactions*, Academic Press, New York, NY, 1967, p. 287.
28 A. M. Clogston, V. Jaccarino and Y. Yafet, *Phys. Rev. A*, *134* (1964) 650.
29 A. J. Freeman and R. E. Watson, in R. T. Rado & H. Suhl (eds.), *Magnetism*, Vol. IIA, Academic Press, New York, NY, 1965, p. 167.
30 T. Asada and K. Terakura, *J. Phys. F*, *12* (1982) 1387.
31 H. Ebert, J. Abart and J. Voitländer, *J. Phys. F*, *16* (1986) 1287.
32 A. Narath, *Phys. Rev.*, *162* (1967) 320.